Ultradeep near-infrared imaging of HDF-south: rest-frame optical properties of high redshift galaxies

Ivo Labbe, Marijn Franx, Gregory Rudnick, Alan F. M. Moorwood, Natascha Foerster Schreiber, et al.

Ivo Labbe, Marijn Franx, Gregory Rudnick, Alan F. M. Moorwood, Natascha Foerster Schreiber, Hans-Walter Rix, Lottie van Starkenburg, Peter van Dokkum, Paul P. van der Werf, Huub J. A. Roettgering, Konrad Kuijken, "Ultradeep near-infrared imaging of HDF-south: rest-frame optical properties of high redshift galaxies," Proc. SPIE 4834, Discoveries and Research Prospects from 6- to 10-Meter-Class Telescopes II, (13 February 2003); doi: 10.1117/12.457539

SPIE.

Event: Astronomical Telescopes and Instrumentation, 2002, Waikoloa, Hawai'i, United States

Ultradeep near-infrared imaging of the HDF-South: rest-frame optical properties of high redshift galaxies

Ivo Labbé[a], Marijn Franx[a], Gregory Rudnick[b], Alan Moorwood[c], Natascha Förster Schreiber[a], Hans-Walter Rix[d], Lottie van Starkenburg[a], Peter van Dokkum[e], Paul van der Werf[a], Huub Röttgering[a] and Konrad Kuijken[a]

[a]Leiden Observatory, Niels Bohrweg 2, Leiden, The Netherlands
[b]Max-Plank-Institut für Astrophysik, Karl-Schwarzschild-Str. 1, Garching, Germany
[c]European Southern Observatory, Karl-Schwarzschild-Str. 2, Garching, Germany
[d]Max-Plank-Institut für Astronomie, Königstuhl 17, Heidelberg, Germany
[e]California Institute of Technology, 1200 East California Boulevard, Pasadena (CA), USA

ABSTRACT

We have obtained ultradeep J_s, H and K_s near-infrared imaging of the Hubble Deep Field South WFPC2 field with the ISAAC camera on the VLT. The total integration time of 100 hours resulted in the deepest ground-based infrared observations to date and the deepest K_s-band data ever taken. This depth allows us to determine the spectral energy distributions of the high-redshift galaxies with unprecendented accuracy. Together with existing optical observations, we use the multicolor data to select high-redshift galaxies by their rest-frame optical light, and study their statistical properties and morphologies. We find a wide variety of morphologies: some are large in the rest-frame optical and resemble normal spiral galaxies, others are barely detected in the observers optical and have red NIR colors. The latter belong to a new population of galaxies at redshifts $z > 2$, that is notably absent in the HDF-North. The spectral energy distributions of many of such red galaxies show distinct breaks, which we identify as the balmer break/4000 Angstrom break, and their contribution to the stellar mass density is estimated to be substantial. At redshift $z \sim 3$, we find a clear excess of superluminious galaxies ($> 5 \times L_B^*(z = 0)$), which is consistent with 1 magnitude of luminosity evolution. Overall, the results show the necessity of deep near-infrared imaging to obtain a full census of the high redshift universe.

Keywords: large telescopes, near infrared imaging, high redshift galaxies, galaxy evolution, galaxy morphology, luminosity functions

1. INTRODUCTION

In the past decade, our ability to routinely identify and systematically study distant galaxies has dramatically advanced our knowledge of the high-redshift universe. In particular, the effective U-dropout technique[1,2] has enabled us to select distant galaxies using simple photometric criteria. Now more than 1000 of these Lyman break galaxies (LBGs) are spectroscopically confirmed at $z > 2$, and they have been subject to targeted studies on spatial clustering,[3] internal kinematics,[4,5] dust properties,[6] and stellar composition.[7,8] Although LBGs are among the best studied classes of distant galaxies to date, many of their properties are still unknown.

More importantly, it is unclear if the ultraviolet-optical selection technique alone will give us a fair census of the galaxy population at $z \sim 2 - 3$ as it requires high-redshift galaxies to have high far-ultraviolet surface brightnesses and blue observed optical colors. We know there exist highly obscured active galaxies, detected in the sub-mm and radio-surveys,[9] and optically faint hard X-ray sources[10,11] at high redshift that would not be selected this way, but their number densities are lower compared to LBGs and they might represent rare populations or transient evolutionary phases. However, even present-day elliptical and spiral galaxies if

Further author information: (Send correspondence to I.L.)
I.L.: E-mail: ivo@strw.leidenuniv.nl, Phone: +31 71 527 5805, Fax: +31 71 527 5743, Postal address: P.O. Box 9513, NL-2300 RA, Leiden, The Netherlands

Discoveries and Research Prospects from 6- to 10-Meter-Class Telescopes II, Puragra Guhathakurta, Editor, Proceedings of SPIE Vol. 4834 (2003) © 2003 SPIE · 0277-786X/03/$15.00

placed at high redshift would not satisfy the U-dropout criteria because most of them would be too faint in the rest-frame UV. In such cases, the addition of near-infrared (NIR) bands is crucial because it allows to access the familiar rest-frame optical emission of objects at redshifts $1 < z < 4$. This enables comparison of galaxies of different epochs at wavelengths where long-lived stars may dominate the integrated light, thus tracing the build-up of stellar mass directly.

In this context we initiated the Faint InfraRed Extragalactic Survey (FIRES)[12]; a large public program consisting of very deep near-infrared (NIR) imaging of two fields, carried out at the *Very Large Telescope* (VLT), to access the rest-frame optical emission of objects at redshifts $2 < z < 4$. We observed fields with existing deep optical WFPC2 imaging from the *Hubble Space Telescope* (HST): the WPFC2 main-field of Hubble Deep Field South, and the field around the distant cluster MS1054-03. By selecting sources in the near-infrared K_s-band, we hope to obtain a more complete view of the high-redshift universe. Compared to the rest-frame far-UV, rest-frame optical light is less sensitive to the effects of dust extinction and on-going star formation, and provides a better tracer of stellar mass. The extended wavelength coverage ($0.3 - 2.2\mu$m) is required not only to access the rest-frame optical, but also to determine the redshifts of faint galaxies from their broadband photometry alone.

We present here selected results of the HDF-S. The observations, reduction and analysis techniques are described in detail in Ref. 13 and Ref. 14; the results on MS1054-03 will be presented in Ref. 15. Throughout this paper, we assume a flat Λ-dominated cosmology ($\Omega_M = 0.3, \Lambda = 0.7, h = H_0/100$ km s^{-1} Mpc^{-1} $= 1.0$). Unless explicitly stated otherwise, all magnitudes are expressed in the Johnson[16] photometric system.

2. OBSERVATIONS AND PHOTOMETRY

The NIR observations of the HDF-S were obtained using the Infrared Spectrograph and Array camera[17] (ISAAC) on the VLT/ANTU at Paranal. The ISAAC field of view is $2.5' \times 2.5'$ with a pixel scale of $0.147''$pixel^{-1}. We dithered many exposures in the J_s (1.24μm), H (1.65μm) and K_s (2.17μm) bands, with individual exposure times of 120s, 120s, and 60s, respectively. The total integration time in each passband is about 33 hours and the median seeing of all infrared frames is about $0.46''$. In the deepest central $2.1' \times 2.1'$, we reach total AB magnitudes for point sources of 25.9, 24.8 and 24.4 in J_s, H, and K_s, respectively (3σ signal-to-noise). The details of the reduction and photometry will be presented in Ref. 13.

We complemented the ISAAC data with HST/WFPC2 imaging[18] (version 2) in the filters $F300W$, $F450W$, $F606W$ and $F814W$, which are close to the U, B, V and I bands, respectively. We constructed a K_s-band selected sample of galaxies and measured colors in all seven passbands within the K_s-detection isophote using the SExtractor software,[19] after accounting for differences in resolution and image quality between the HST and VLT data set. Finally we determined the photometric redshifts and associated uncertainties of all extragalactic sources using a method detailed in Ref. 24. The depth of the current survey allows us to determine the spectral energy distributions of the high-redshift galaxies with unprecendented accuracy, which is necessary for reliable photometric redshifts and a proper understanding of stellar populations of the high-redshift galaxies.

3. NIR PROPERTIES OF LYMAN BREAK GALAXIES

The LBGs identified in our K_s-band selected catalogue are different from those found in previous surveys, showing a large variation in both morphologies and spectral energy distributions (SEDs). We selected them by applying the criteria of Madau et al.[20] While most U-dropouts are compact at all wavelengths, some are large in the rest-frame optical and show profound differences between the rest-frame ultraviolet and optical morphologies, as shown in Fig. 1.

The I-band morphologies (rest-frame $2000 - 2700$ Å) are complex with knotty structure, whereas the NIR light is more centrally concentrated and extended, reminiscent of red bulges and bluer disks with star-forming clumps. In a few cases the rest-frame optical light is almost spatially distinct from the far-ultraviolet. The change in morphology when moving to the NIR is not dominated by the decreasing resolution of the ground-based data but reflects a change in the physical distribution of the light. These properties are in stark contrast with the compact and small sizes traditionally emphasized,[21,22] and the segregated UV-optical morphology has

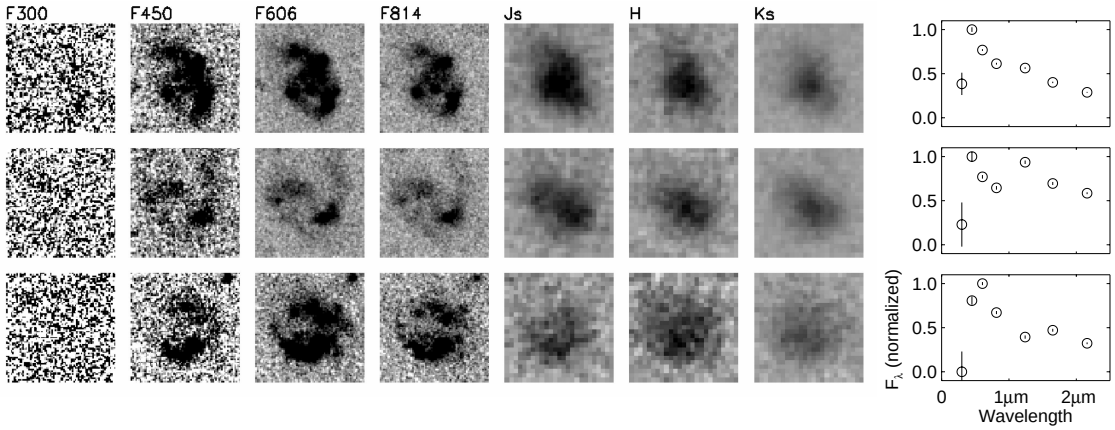

Figure 1. Morphology of the most extended U-drop galaxies in the HDF-S. The left panels show the WFPC2 U, B, V, I data, and right hand panels show our VLT/ISAAC J_s, H, K_s data. The images are 3 x 3 arcsec on a side. The intensity is proportional to F_λ, with arbitrary normalization for each galaxy. The right hand column shows the spectral energy distributions. As can be seen, these U-drop galaxies are large in extent, and can show prominent Balmer breaks. The K-band infrared images (rest-frame optical) are generally more centrally concentrated than the WFPC2 images; this is a physical change and not caused by the difference in image quality. The galaxy in the bottom row is spectroscopically confirmed at $z_{spec} = 2.8$.

not been seen in the HDF-N.[25] The LBGs with complex structures are amongst the brightest and reddest in the rest-frame optical, suggesting higher mass-to-light ratios, and they might be the most massive LBGs around. Their spectral energy distributions show a pronounced break in the rest-frame optical, which we identify as the age-sensitive Balmer/4000 Å break. Follow-up VLT/FORS spectroscopy[23] confirmed the redshift for one of the large galaxies, a disk-like U-dropout at $z_{spec} = 2.793 \pm 0.003$, implying a physical diameter of 10 h^{-1} kpc. While this is only one example, models of galaxy formation must produce objects of comparable sizes and in sufficient numbers to be consistent with our observations.

4. BALMER BREAK GALAXIES

Evolved quiescent galaxies with a prominent Balmer discontinuity in the spectrum, like most present-day Hubble Type galaxies, would have very red observed NIR colors if placed at redshifts $z > 2$, and extremely faint in the observed optical. In the HDF-S we find a substantial population of such red galaxies with $J_s - K_s > 2.3$ and photometric redshifts $2 < z_{phot} < 4$. These galaxies are generally compact, with exceptions, as can be seen in Fig. 2. Most of them are extremely faint in the observed optical with red $V_{606} - H$ colors, and would be missed by the standard U-dropout criteria.

Whether the red NIR colors are due to age or dust has not been determined for the sample as a whole, but many spectral energy distributions exhibit a clear break between the J_s and H bands, more consistent with a Balmer/4000 Å break. One of the galaxies shows extremely red NIR colors similar to the curious "J-dropout" HDF-N JD1,[26] possibly a maximally old elliptical or highly reddened galaxy at $z \sim 3$. Another shows an H-band surface brightness profile which can be fit with an exponential out to 1″ radius and this galaxy seems to host an arc of blue knots in the WFPC2 images; possibly star-forming sites embedded in a larger evolved system. .

We find 13 red objects having $K_{J,tot} < 22$ compared to 37 U-dropouts to the same flux limit. Interestingly, the contribution of K_s-band light and the red rest-frame optical colors suggest this red population contains a significant fraction of the total stellar mass at this cosmic epoch. The surface density of these red sources is not well known; the HDF-N has far fewer red galaxies than the HDF-S, as is apparent from comparing Fig. 3 to Fig 1. in Ref. 7 which shows a similar plot of a NIR selected sample in the HDF-N. In the same diagram, we find 7 galaxies redder than $V_{606,AB} - H_{AB} > 3$ and brighter than $H_{AB} < 25$, compared to one in the HDF-N.

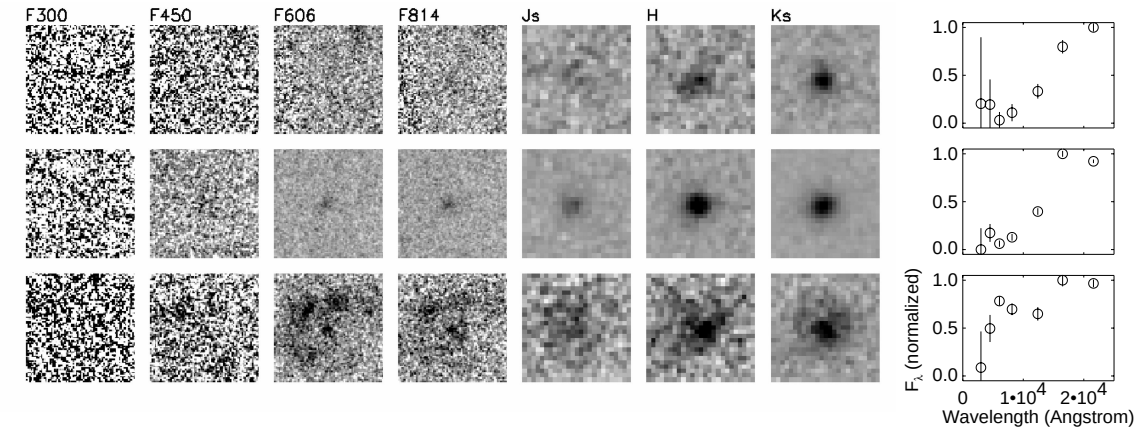

Figure 2. same as Fig. 1, but for some of the red galaxies. Many of these galaxies are small, and show prominent breaks in the infrared (rest-frame optical). Note that the galaxy in the top row is barely visible even in J_s. The SED of the object in the middle is consistent with a strong Balmer break at $z \sim 2.5$. The galaxy in the bottom row is very extended in the rest-frame optical. It shows faint emission in the H-band out to $1''$, consistent with an exponential profile.

5. OPTICAL LUMINOSITY EVOLUTION AT $2 < Z < 3.5$

Our long wavelength baseline allows us to observe the B-band rest-frame wavelength over a large range in redshift. From the best-fit SED at the best-fit redshift, we measured the rest-frame luminosity in the B-band for our galaxies and plot this as a function of enclosed volume and redshift in Fig. 4. Details of the photometric redshifts determination and rest-frame luminosity calculation can be found in Ref. 24. We find a clear excess of superluminous galaxies and redshifts between $2 < z < 3.5$. Where no-evolution scenarios, using local luminosity functions from SDSS[28] and 2dFGRS,[29] predict ≈ 0.1 galaxies with $L_B > 5 \times L^*_{B,rest}(z = 0)$ for the volume probed by our data, we find nine such galaxies. Although random errors in the photometric redshift will tend to produce a bias in the derived luminosities, since the luminosity function declines very steeply towards higher luminosities and the smoothing will increase the number of observed very luminous galaxies, we estimate that this effect is limited. Furthermore, the first spectroscopic observations have confirmed the existence of these luminous galaxies.[23] However, because of the small comoving volumes enclosed in this redshift range, these numbers may not be indicative of the galaxy population as a whole.

If L^*_B is increased by a factor of 2.7 or 3.2 for the SDSS and 2dFGRS luminosity functions, about one magnitude a luminosity evolution in the B-band, then nine galaxies are predicted. Pure luminosity evolution models[27] could easily account for such brightening, but current models do not take into account absorption by dust in the galaxies, or any of the observational biases or the incompleteness that may occur for IR-selected galaxies. While NIR selection is generally thought to be less prone to extinction effects and less dependent on the current SFR than optical selection, surface brightness dimming and the bright IR sky can limit detection efficiency for extended objects. We note that Shapley et al.[8] also studied the IR properties of U-dropouts and found their rest-frame optical luminosity function greatly exceeding locally determined values. However, an important distinction with our work is that they studied a rest-frame UV selected sample using only limited IR passbands.

6. CONCLUSIONS

The first results of the HDF-S demonstrate the necessity of extending optical observations to near-IR wavelengths for a more complete census of the early universe. Our deepest K_s-band proves invaluable for it probes well into the rest-frame optical at $2 < z < 4$, where long-lived stars may dominate the light of galaxies. We find:

- high-redshift systems that are very extended in the rest-frame optical with complex UV morphologies. Some have spatially distinct rest-frame UV and optical light distributions, where in general the rest-frame

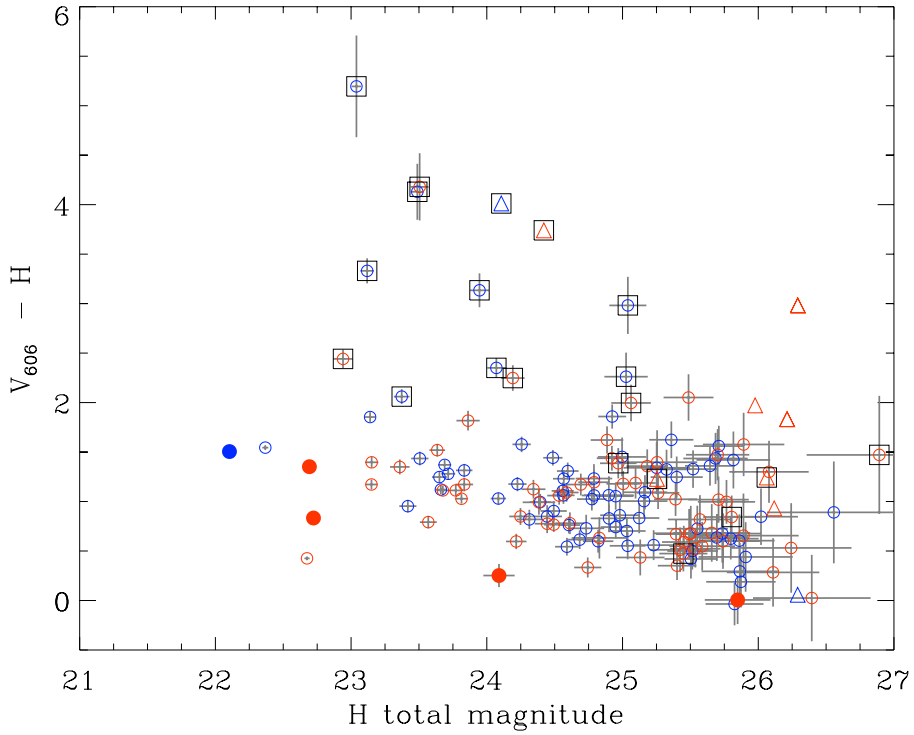

Figure 3. $V_{606} - H$ versus H color-magnitude diagram (on the AB system) for galaxies in the K_s-selected catalog of the HDFS that are photometrically at $1.95 < z_{phot} < 3.5$. Filled symbols indicate galaxies with spectroscopy, and the data points are grouped into two redshift ranges: $1.95 \leq z < 2.7$ *(red)* and $2.7 \leq z \leq 3.5$. The number of candidates for red, evolved galaxies is much higher than in the HDF-N, as shown in a identical plot in Fig. 1 in Ref.[7]: we find 7 galaxies redder than $V_{606,AB} - H_{AB} > 3$ and brighter than $H_{AB} < 25$, compared to one in the HDF-N. For easy comparison, we give the magnitudes and colors in the AB system, where $V_{606,AB} = V_{606} + 0.12$ and $H_{AB} = H + 1.38$. Galaxies with S/N < 2 for the V_{606} measurement (*triangles*) are plotted at the 2σ confidence limit in V_{606}, indicating a lower limit on the $V_{606} - H$ color. The subsample of galaxies having red $J_s - K_s > 2.3$ colors (*open squares*) are also indicated.

optical is more centralized. Some of them have disky structure with clumps of star formation, similar to local spiral galaxies.

- a previously undiscovered population of red galaxies with $(J_s - K_s > 2.3)$ at $z > 2$. Because most of them are barely detectable even in the deepest optical images, they would be missed by ultraviolet-optical color selection techniques, such as the U-dropout method. Many of these galaxies show a prominent jump in the NIR, which may be caused by the Balmer/4000 Å break. The red galaxies likely contribute significantly to the total stellar mass budget at redshifts $z \sim 3$.

- a clear excess of luminous galaxies with rest-frame luminosties of $L_B > 5 \times h^{-2} L^*_{B,rest}(z = 0)$ at $2 < z < 3.5$, consistent with a luminosity brightening of one magnitude in the B-band compared to present-day values.

We are pursuing our follow-up program to obtain more spectroscopic redshifts needed to confirm the above results. It remains surprising that the first results of the HDF-S are so different compared to what has been found in the HDF-N, yet both fields are rather small and results based on them may be seriously affected by large scale structure in the universe. This calls for more observations to similar limits with full optical-to-infrared coverage.

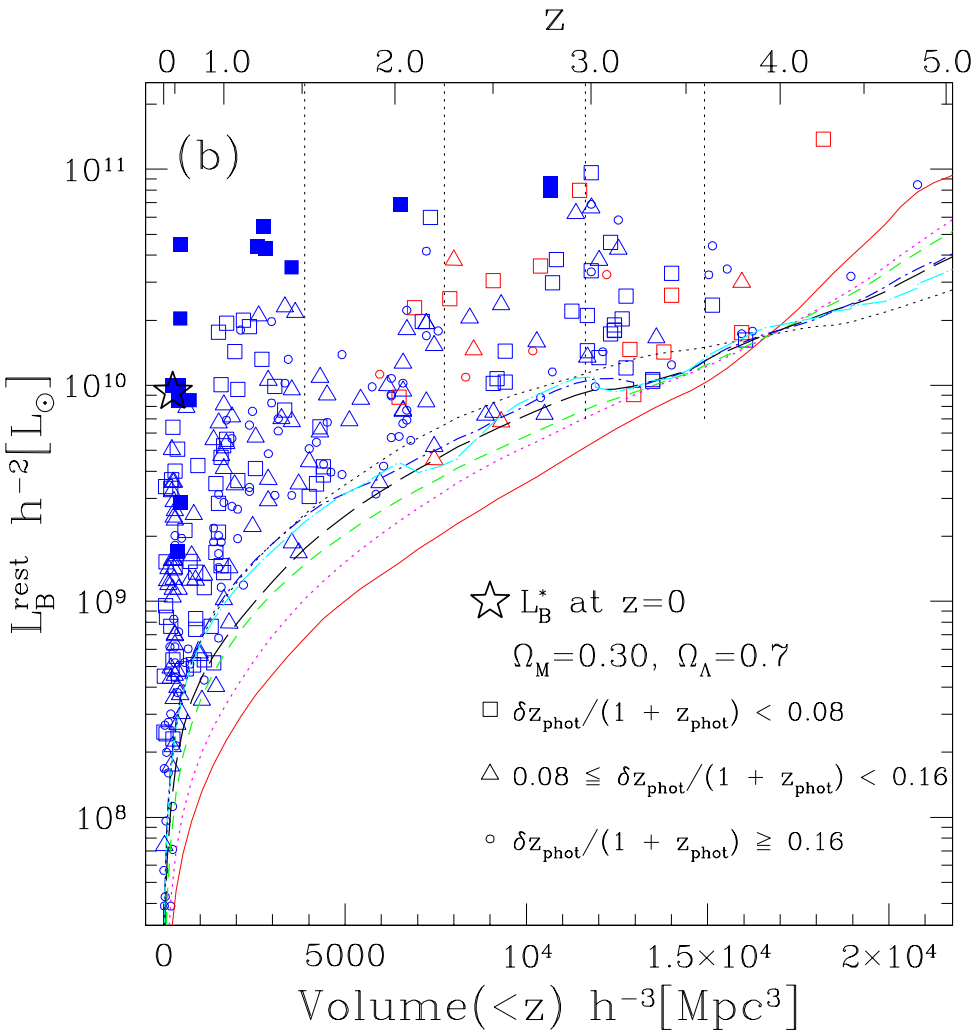

Figure 4. The distribution of rest-frame B-band luminosities as a function of enclosed co-moving volume and photometric redshift z_{phot}. We show all galaxies with $K_{s,tot} < 23$. Galaxies which have spectroscopic redshifts are represented by solid points. Note the presence of galaxies at $z_{phot} \geq 2$ with $L_B \geq 5 \times 10^{10} L_\odot$. The tracks represent the values of L_B for each of our seven template spectra normalized at each redshift to $K_{s,tot} = 23$. The large star indicates the value of L_B^* from local surveys. The point shape indicates the photometric redshift reliability with the point color corresponding to the $J_s - K_s$ color: galaxies with $J_s - K_s < 2.3$ are shown in blue, galaxies with $J_s - K_s > 2.3$ in red. The specific tracks correspond to the E (*solid*), Sbc (*dot*), Scd (*short dash*), Irr (*long dash*), SB1 (*dot–short dash*), SB2 (*dot–long dash*), and 10MY (*dot*) templates.

ACKNOWLEDGMENTS

We would like to thank the ESO staff for their assistance and their hard efforts in taking these data and making them available to us.

REFERENCES

1. Steidel, C. C., Giavalisco, M., Dickinson, M., & Adelberger, K. L., "Spectroscopy of Lyman Break Galaxies in the Hubble Deep Field," *AJ* **112**, pp. 352–358, 1996

2. Steidel, C. C., Giavalisco, M., Pettini, M., Dickinson, M., & Adelberger, K. L., "Spectroscopic confirmation of a population of normal star-forming galaxies at redshifts $Z > 3$," *ApJ* **462**, L17, 1996
3. Giavalisco, M. & Dickinson, M., "Clustering segregation with ultraviolet luminosity in Lyman Break Galaxies at $z \sim 3$ and its implications," *ApJ* **550**, pp. 177–194, 2001
4. Pettini, M., Kellogg, M., Steidel, C. C., Dickinson, M., Adelberger, K. L., & Giavalisco, M., "Infrared observations of nebular emission lines from galaxies at $Z \sim 3$," *ApJ* **508**, pp. 539–550, 1998
5. Pettini, M., Shapley, A. E., Steidel, C. C., Cuby, J., Dickinson, M., Moorwood, A. F. M., Adelberger, K. L., & Giavalisco, M., "The rest-frame optical spectra of Lyman Break Galaxies: star formation, extinction, abundances, and kinematics," *ApJ* **554**, pp. 981–1000, 2001
6. Adelberger, K. L. & Steidel, C. C., "Multiwavelength observations of dusty star formation at low and high redshift," *ApJ* **544**, pp. 218–241, 2000
7. Papovich, C., Dickinson, M., & Ferguson, H. C., "The stellar populations and evolution of Lyman Break Galaxies," *ApJ* **559**, pp. 620–653, 2001
8. Shapley, A. E., Steidel, C. C., Adelberger, K. L., Dickinson, M., Giavalisco, M., & Pettini, M., "The rest-frame optical properties of $z \sim 3$ galaxies" *ApJ* **562**, pp. 95–123, 2001
9. Smail, I., Ivison, R. J., Owen, F. N., Blain, A. W., & Kneib, J.-P., "Radio constraints on the identifications and redshifts of submillimeter galaxies," *ApJ* **528**, pp. 612–616, 2000
10. Cowie, L. L. et al., "Detecting high-redshift evolved galaxies as the hosts of optically faint hard X-ray sources," *ApJ* **551**, L9, 2001
11. Barger, A. J., Cowie, L. L., Bautz, M. W., Brandt, W. N., Garmire, G. P., Hornschemeier, A. E., Ivison, R. J., & Owen, F. N., "Supermassive black hole accretion history inferred from a large sample of chandra hard X-ray sources," *AJ* **122**, pp. 2177–2189, 2001
12. Franx, M. et al., "FIRES at the VLT: the Faint InfraRed Extragalactic Survey," *The Messenger* **99**, pp. 20–22, 2000
13. Labbe, I. F. L. et al., "Ultradeep near-infrared ISAAC observations of the Hubble Deep Field South: observations, reduction, multicolor catalog and photometric redshifts," in preparation, 2002
14. Rudnick, G. et al., "A K-band selected photometric redshift catalog in the Hubble Deep Field South: sampling the rest-frame V band to $z = 3$," *AJ* **122**, pp. 2205–2221, 2001
15. Förster Schreiber, N.M. et al., "Deep near-infrared ISAAC observations of the cluster MS1054–03," in preparation, 2002
16. Johnson, H. L., "Astronomical measurements in the infrared", *ARA&A* **4**, pp. 193–206, 1966
17. Moorwood, A. F., "ISAAC: a 1-5 um imager/spectrometer for the VLT," in *Optical telescopes of today and tomorrow*, A. L. Ardeberg ed., *proc. SPIE* **2871**, pp. 1146–1151, 1997
18. Casertano, S. et al., "WFPC2 observations of the Hubble Deep Field South," *AJ* **120**, pp. 2747–2824, 2000
19. Bertin, E. & Arnouts, S., "SExtractor: software for source extraction," *A&AS* **117**, 393, 1996
20. Madau, P., Ferguson, H. C., Dickinson, M. E., Giavalisco, M., Steidel, C. C., & Fruchter, A., "High-redshift galaxies in the Hubble Deep Field: colour selection and star formation history to $z \sim 4$," *MNRAS* **283**, pp. 1388–1404, 1996
21. Giavalisco, M., Steidel, C. C., & Macchetto, F. D., "Hubble Space Telescope imaging of star-forming galaxies at redshifts $Z > 3$," *ApJ* **470**, 189, 1996
22. Lowenthal, J. D. et al.,"Keck spectroscopy of redshift z approximately 3 galaxies in the Hubble Deep Field," *ApJ* **481**, pp. 673–688, 1997
23. Rudnick, G. et al., "Spectroscopy of K_s-band selected galaxies in the Hubble Deep Field South," in preparation, 2002a
24. Rudnick, G. et al., "The rest-frame optical luminosity density of K_s-band selected galaxies from $z = 0$ to $z = 4$," in preparation, 2002b
25. Dickinson, M., "The first galaxies: structure and stellar populations" *Philos. Trans. R. Soc. London* **A 358**, p. 2001, 2000
26. Dickinson, M. et al., "The unusual infrared object HDF-N J123656.3+621322," *ApJ* **531**, pp. 624–634, 2000

27. Kauffmann, G. & Charlot, S., "The K-band luminosity function at $z = 1$: a powerful constraint on galaxy formation theory," *MNRAS* **297**, L23, 1998
28. Blanton, M. R. et al., "The luminosity function of galaxies in SDSS commissioning data," *AJ* **121**, pp. 2358–2380, 2001
29. Folkes, S. et al., "The 2dF Galaxy Redshift Survey: spectral types and luminosity functions," *MNRAS* **308**, pp. 459–472, 1999